PROCEEDINGS OF THE SIXTEENTH LUNAR AND PLANETARY SCIENCE CONFERENCE, PART 2
JOURNAL OF GEOPHYSICAL RESEARCH, VOL. 91, NO. B4, PAGES D344–D354, MARCH 30, 1986

A Compositional Study of the Aristarchus Region of the Moon Using Near-Infrared Reflectance Spectroscopy

P. G. LUCEY[1], B. R. HAWKE[1], C. M. PIETERS[2], J. W. HEAD[2], T. B. MCCORD[1]

Newly obtained near-infrared reflectance spectra for features on or near the Aristarchus Plateau demonstrate the diversity of compositions in the region. Highland units are of three probable compositions: a feldspar and clinopyroxene assemblage; a probable clinopyroxene, olivine, and possibly feldspar assemblage; and an assemblage composed of olivine or olivine and feldspar. The feldspar-clinopyroxene assemblage is tentatively correlated with the major Th anomaly centered on Aristarchus crater. The regional pyroclastic deposits on the plateau are composed of greater than 90% Fe^{2+}-bearing glass. The Aristarchus cratering event fully penetrated any mare or pyroclastics in the target. Evidence for mare-related material is found in the ejecta on the mare side of the mare-plateau contact.

I. INTRODUCTION

The Aristarchus region is one of the most geologically complex areas on the moon and contains a variety of spectral, geochemical, radar, and thermal anomalies [e.g., *Zisk et al.*, 1977]. The region is dominated by the Aristarchus Plateau, a rectangular, elevated crustal block about 170 × 220 km (Figures 1 and 2) that is blanketed by varying thicknesses of dark mantling material of probable pyroclastic origin and is embayed by the mare basalts of Oceanus Procellarum. The relatively fresh Copernican crater Aristarchus, 40 km in diameter, straddles the boundary between mare and plateau at the southeastern edge of the plateau.

The Aristarchus region has long attracted the attention of lunar scientists. *Wood* [1912] pointed out the existence of a spectral anomaly and indicated that a portion of the region exhibited the lowest ultraviolet albedo of the lunar nearside. In the most recent summary of photogeologic and remote sensing data for the Aristarchus region, *Zisk et al.* [1977] noted that in addition to its low albedo and red color, the Aristarchus Plateau is characterized by (1) the lowest 3.8-cm and 70-cm radar reflectivity values observed for any large lunar area [*Zisk et al.*, 1977 *Thompson*, 1979], (2) an unusually low eclipse temperature [*Shorthill and Saari*, 1965], (3) very high concentrations of radioactive elements in the vicinity of Aristarchus crater [*Haines et al.*, 1979], (4) high radon emanations in the vicinity of Aristarchus [*Gorenstein and Bjorkholm*, 1973], and (5) numerous transient phenomena reported for the plateau [e.g., *Cameron*, 1971]. *Davies et al.* [1979] presented infrared spectral ratio images that suggested that the dark mantling material in the Aristarchus region was composed of pyroclastic glasses that were unlike those sampled by the Apollo 17 mission. The most recent Th deconvolution modeling [*Etchegaray-Ramirez et al.*, 1982] has demonstrated that Aristarchus crater exposed Th-rich (18–22 ppm) material.

Although the region has been the subject of numerous remote sensing and geologic investigations [e.g., *Moore*, 1965, 1967; *Guest*, 1973; *Zisk et al.*, 1977; *Davies et al.*, 1979; *Etchegaray-Ramirez et al.*, 1982; *Guest and Spudis*, 1985] the composition, origin, and evolution of the observed geologic units are not fully understood. The purpose of this study is to use newly obtained near-infrared spectral data to investigate the composition and distribution of surface material in the Aristarchus region.

II. ASTRONOMICAL OBSERVATIONS

Near-infrared reflectance spectra were obtained of several spots in and around Aristarchus crater and on the Aristarchus Plateau with the Planetary Geosciences Division indium antimonide infrared CVF spectrometer at the University of Hawaii 2.24-m telescope at Mauna Kea Observatory. The spectrometer succesively measures intensity in each of 120 wavelength channels in the 0.6–2.5-range by rotating a filter with continuously variable bandpass. Each of the lunar spots was observed independently two or three times within a 1.5-h sequence. Some of the Aristarchus observations were made with a 2.3-arcsec aperture at a focal ratio of f/10 that isolated a 4.3 × 8.4 km ellipse on the lunar surface for spectrophotometer measurements. Other spectra were 4obtained using increased magnification at f/35 for which the aperture subtends 0.7 arcsec, allowing spectra to be obtained for 1.6 × 3.1 km spots under optimum observing conditions.

Frequent observations were made of the Apollo 16 landing site and other lunar reflectance standard areas. These observations were used to monitor the atmospheric extinction throughout each night. Extinction corrections were made using the interactive computer program presented by *Clark* [1979], producing spectra representing the reflectance ratio between the observed areas and the Apollo 16 landing site. The reflectance curve of the carefully selected mature Apollo 16 soil sample 62231,1 [*Adams and McCord*, 1972] was used to convert the relative spectra to spectral reflectance. All spectra were scaled to 1.0 at 1.02 μm.

III. SPECTRAL CLASSIFICATION, GEOLOGIC SETTINGS, AND COMPOSITIONAL INTERPRETATION

Spectra were taken of fresh craters or bright features on or near the plateau to determine the compositions of highland material beneath the dark mantle deposits. Very dark, presumably pure, areas of dark mantling material were chosen for observations to determine the nature and composition of this regional dark mantle deposit. Spectra were obtained for the interior and exterior deposits of Aristarchus crater in order

[1]Planetary Geosciences Division, Hawaii Institute of Geophysics
[2]Department of Geological Sciences, Brown University

Paper number 5B7036.
0148-0227/86/005B-7036$05.00

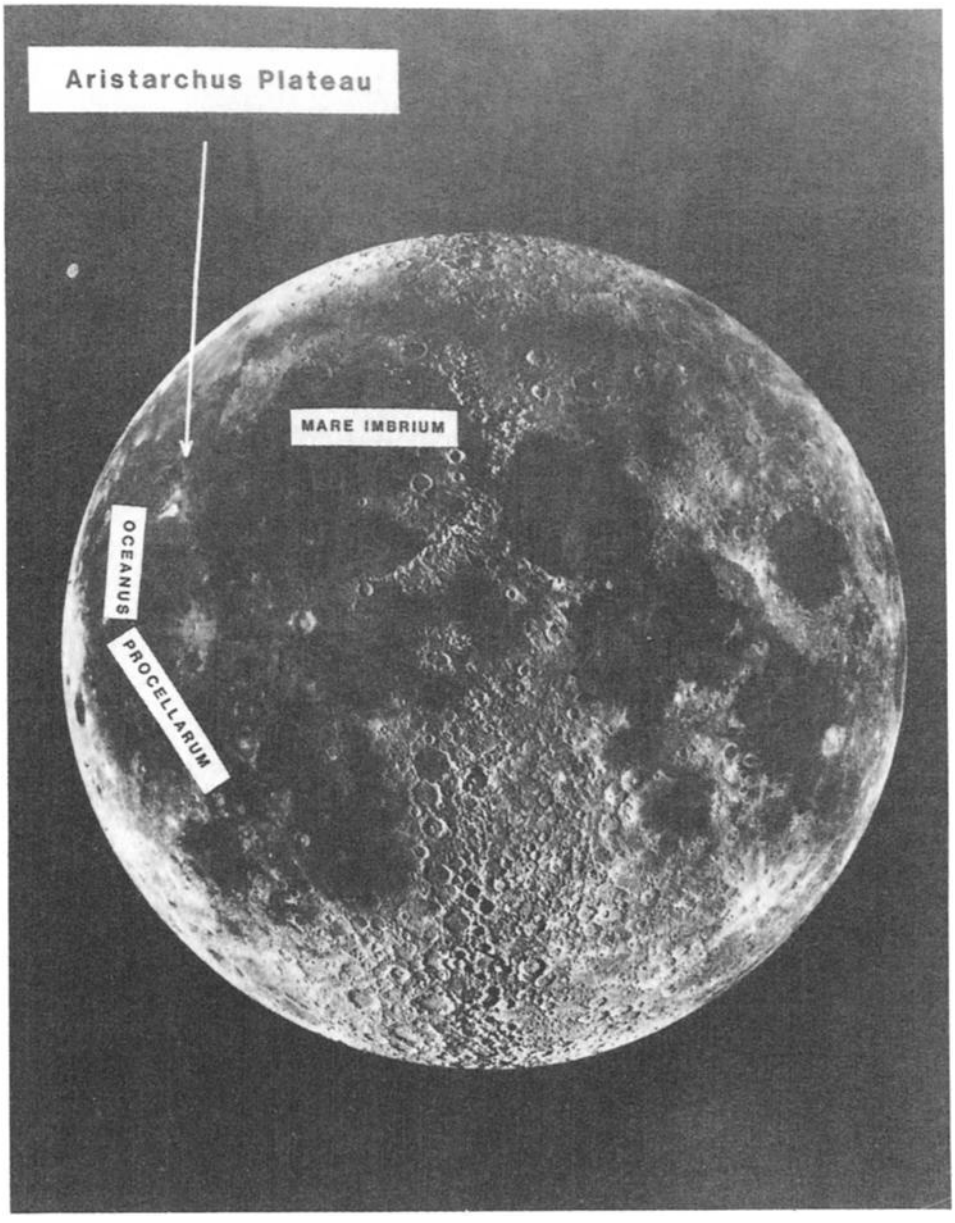

Fig. 1. The location of the Aristarchus Plateau on the nearside of the moon. (Lick Observatory composite)

to investigate the composition and stratigraphy of the target site. Locations of the spots observed are shown in Figure 3. Spectra with acceptable signal-to-noise ratio were collected for 14 areas.

In order to quantitatively classify the data, four spectral parameters were derived for each observed location: (1) the infrared continuum slope, defined as the slope of a straight line drawn through the peaks on either side of the 1-μm absorption and measured as Δ (scaled reflectance) / $\Delta\lambda$; (2) the depth of the absorption, defined as 1 minus the reflectance at the absorption minimum relative to the continuum as defined above; (3) the wavelength of the minimum (parameters 2 and 3 were derived by fitting 15 channels on either side of the absorption minimum with a fourth order polynomial and using this equation to find the relative reflectance and wavelength of the relative minimum absorption); and (4) the width of the absorption derived from the difference in wavelength between the intercepts of the spectrum under analysis and a line parallel to the continuum slope at a relative reflectance equal to half the absorption depth plus the reflectance at the absorption minimum.

The values of these parameters for the spectra are listed in Table 1. Six variation diagrams were made that encompass all the combinations of the parameters. These diagrams are shown in Figure 4.

The reflectance spectra can be grouped into five classes on the basis of the spectral parameters. Each class forms a coherent group in each variation diagram and therefore in the entire parametric space. On Figure 4, the plot of infrared continuum slope versus band width, separates the classes most clearly. Figure 5 shows representative spectra from each class for comparison.

Class 1

Interpretation: feldspar and augite. This group comprises the spectra obtained for the northwest and southwest walls of

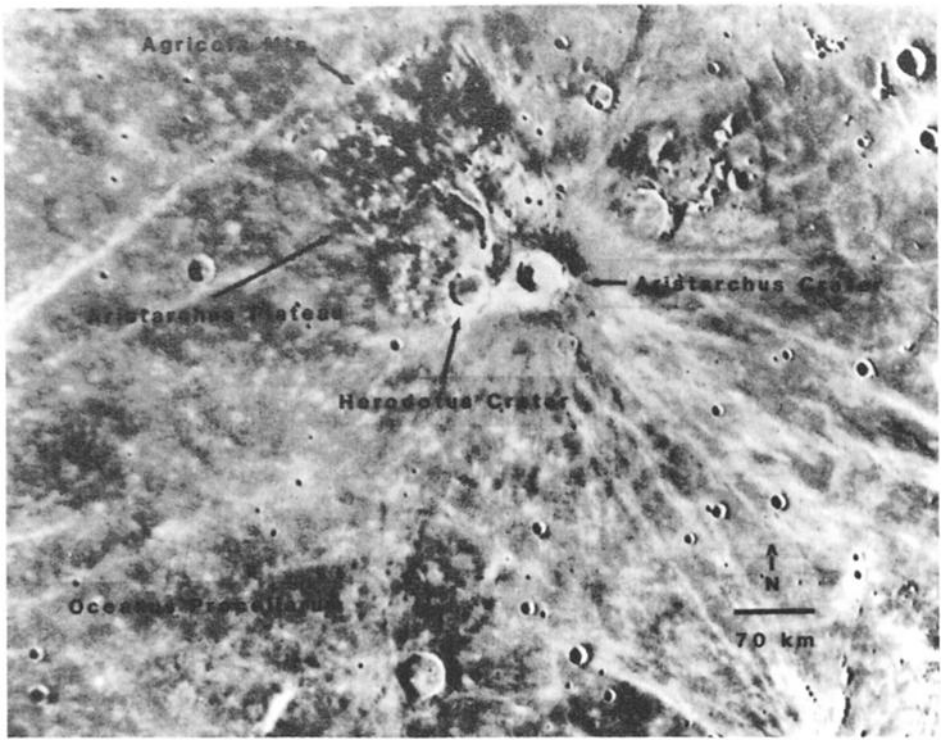

Fig. 2. The Aristarchus Plateau and surroundings. Aristarchus crater is in the southeast corner of the plateau on the contact between plateau and mare. The dark pyroclastic deposits can be easily distinguished on the basis of their low albedo. (Photograph from *Whitaker et al.* [1963], 11-d)

Aristarchus and the small crater Aristarchus A to the north of Aristarchus (Figure 3). The spectra of this class are shown in Figures 6*a,b*. They have deep pyroxene absorptions between 11% and 16% depth with minima occurring between 0.95 and 0.97 μm, distinct shoulders at ~125 μm indicating approximately 2% feldspar absorptions, and shallow continua ranging from 0.21–0.29 ($\Delta R/\Delta\lambda$).

The strong feldspar bands and shallow continuum slopes are diagnostic of feldspar-dominated surface material and indicate that a highland assemblage was excavated by Aristarchus and Aristarchus A. The pyroxene to plagioclase ratio could range from 1–0.1 [*Crown and Pieters*, 1985; *Gaffey*, 1976; *Nash and Conel*, 1974]. The pyroxene chemistry as shown by the wavelength of relative band minima beyond 0.95 μm indicates a high-calcium clinopyroxene component: Ca/Fe + Mg + Ca is 0.3–0.4, indicating an augite [*Adams*, 1974]. This observation is in contrast to most other highland sites, which are dominated by orthopyroxene. The pyroxene absorptions are relatively strong for the spectra of fresh highland terrain, probably due to a greater pyroxene to plagioclase ratio than is typical for highland locations.

Class 2

Favored interpretation: brecciated clinopyroxene and olivine with probable feldspar. The central peak, east wall, and south floor of Aristarchus (Figure 3) have spectra that exhibit broad asymmetric absorptions of 7–8% depth with wavelength minima from ~0.98–0.99 μm (Figures 6*c,d*). These spectra are very similar to each other and show little scatter on the variation diagrams.

Like Class 1, the Class 2 spectra show highland characteristics. The continuum slopes are extremely shallow, exhibiting much lower values than the continua of spectra of mare units and lower even than most highland spectra. This class also contains high-Ca pyroxene, as demonstrated by the absorption features close to 1 μm. The wavelengths of the minima indicate a Ca/Fe + Mg + Ca of 0.4–0.5. This is a maximum value because the 1-μm absorption has been modified by some species that absorbs at longer wavelengths than pyroxene and has probably caused the composite absorption to shift to longer wavelengths. Class 2 differs from Class 1 in that the albedo is in general higher, continuum slopes are shallower, and the absorptions are less deep, broader, asymmetric, and centered at longer wavelengths.

There are four possible interpretations of the composition of Class 2. (1) Extensive brecciation of Class 1 material would increase the albedo and weaken the spectral contrast. However, it would not alter the band center or the symmetry of the absorption. (2) The presence of significant glassy impact melt might cause the changes in band shape observed. However, a recent study of the spectra of impact melt deposits by Smrekar and Pieters (personal communication, 1985) show spectra with very different shapes than those of Class 2. (3) A very low pyroxene to plagioclase ratio would increase the albedo and weaken the pyroxene absorption. However, the difference in band center between the pyroxene present (~0.97 μm) and plagioclase (1.25 μm) would tend to cause splitting of the composite absorption at low pyroxene abundances [*Crown and Pieters*, 1985; *Nash and Conel*, 1974]. The inflection at ~1.2 μm would be enhanced rather than eliminated. (4) The inclusion of abundant olivine would cause the broadening and asymmetry observed at a pyroxene to olivine ratio of about 0.6 [*Gaffey*, 1976]. The high albedo of these locations could be caused either by brecciation or by very abundant feldspar, which is difficult

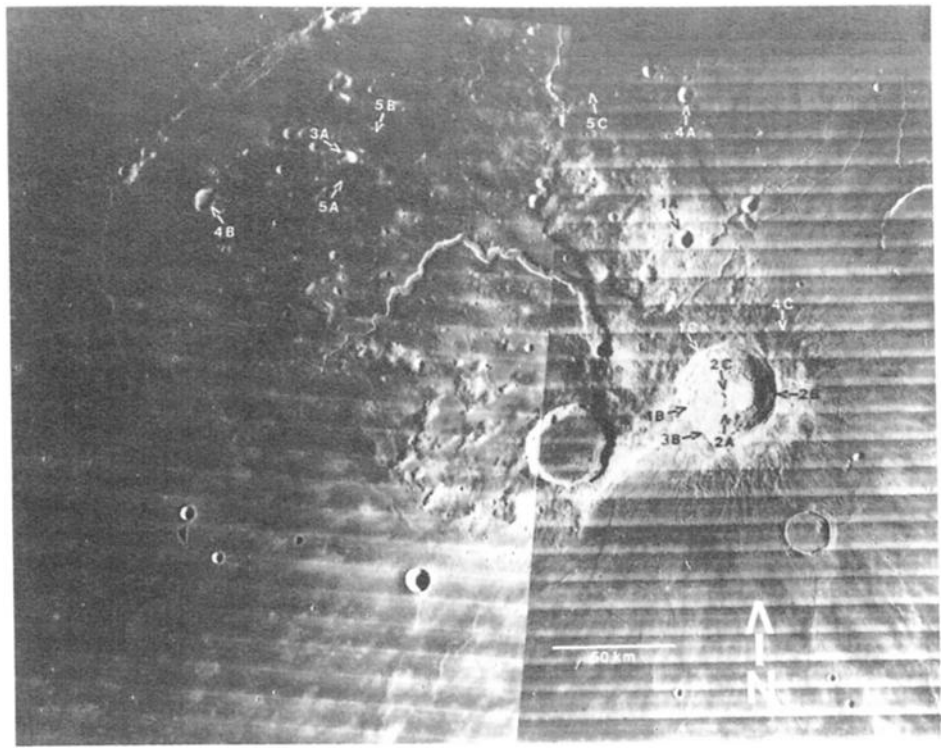

Fig. 3*a*

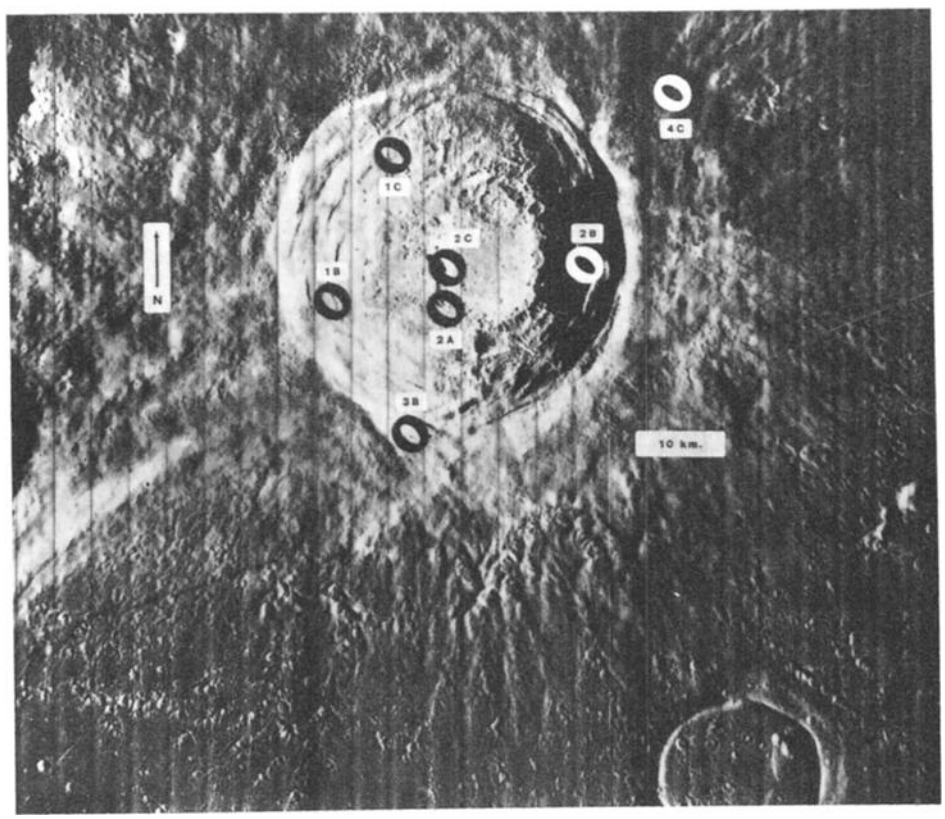

Fig. 3*b*

Fig. 3. (*a*) Spot locations for spectra of the Aristarchus Plateau and region. Numbers and letters denote the spectral class and member to which the spectrum of the spot belong as described in the text and listed in Table 1. (Mosaic of lunar orbiter frames LO IV-150-H3 and LO IV-157-H3) (*b*) Spot locations for spectra of Aristarchus crater interior and immediate surroundings. The ellipses are schematic representations of the actual footprints of the aperture on the lunar surface. The centers of the ellipses correspond to the center of the aperture footprint. The numbers and letters correspond to class numbers and members as above. (Photograph from LO V-197-M)

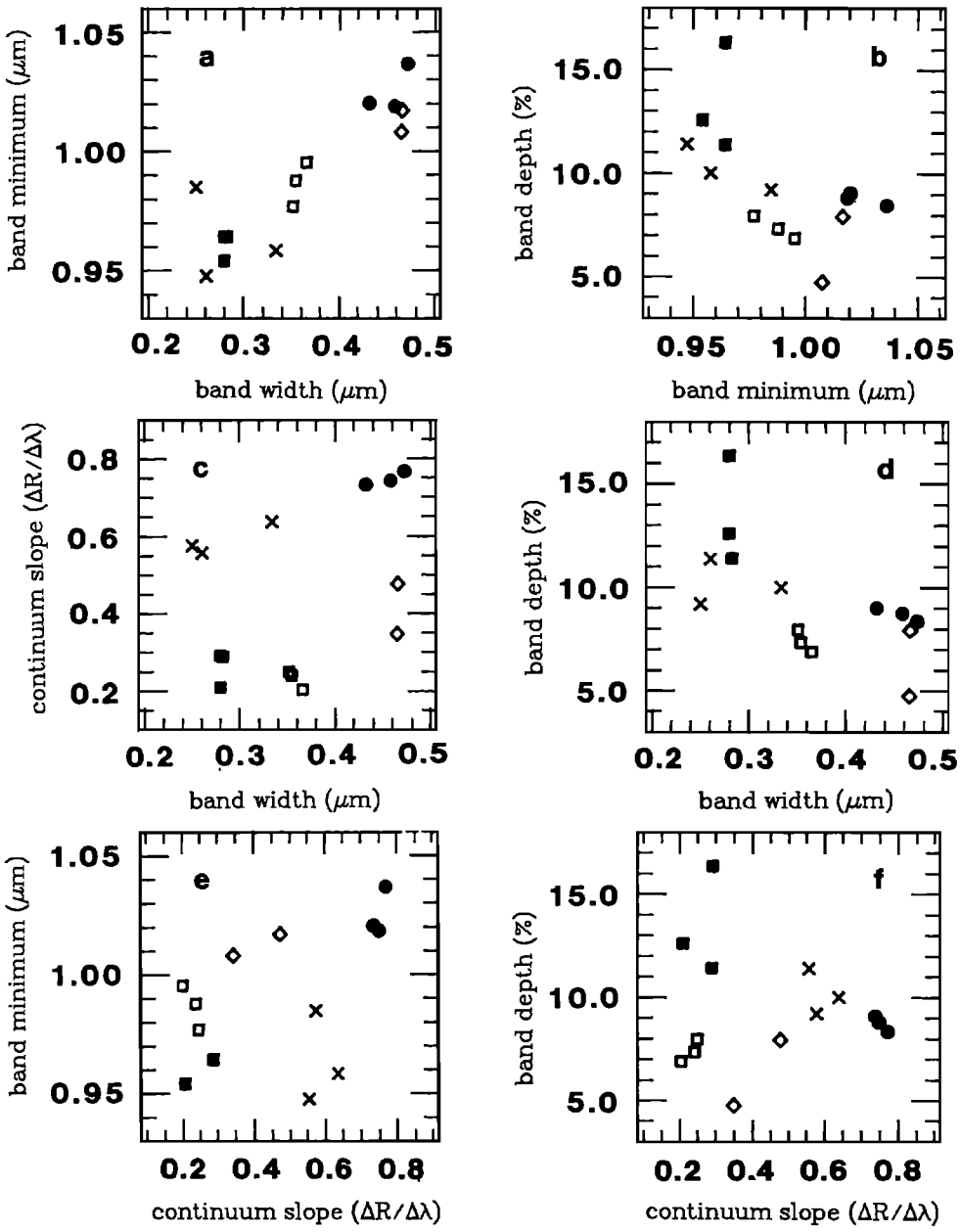

Fig. 4. Variation diagrams derived from the values tabulated in Table 1. Symbols represent the classes listed in the text and in Table 1 as follows: filled squares are Class 1, open squares are Class 2, open diamonds are Class 3, crosses are Class 4, and filled circles are Class 5.

TABLE 1. Spectral Parameters

Class Number and Letter	Location Name	Wavelength of Relative Minimum (μm)	Relative Absorption Depth (%)	Continuum Slope (ΔR/Δλ)	Absorption Width at Half Height (μm)	Mineralogical Interpretation
1A	Aristarchus A	.964	16.3	.290	.280	Feldspar, augite
1B	Aristarchus Southwest Wall	.964	11.4	.288	.283	
1C	Aristarchus Northwest Wall	.954	12.6	.208	.280	
2A	Aristarchus South Floor	.988	7.31	.240	.354	Augite, Olivine, Probable Feldspar
2B	Aristarchus East Wall	.977	7.94	.248	.351	
2C	Aristarchus Central Peak	.995	6.87	.202	.365	
3A	Herodotus X	1.017	7.91	.475	.466	Olivine, Probable Feldspar
3B	Aristarchus South Rim	1.008	4.74	.346	.465	
4A	Aristarchus C	.948	11.39	.556	.261	Mare Mineral Assemblage
4B	Herodotus D	.958	9.99	.637	.334	
4C	Aristarchus Dark Ejecta	.985	9.18	.575	.251	
5A	Aristarchus Plateau 1	1.037	8.407	.768	.472	Fe^{2}-bearing Glass
5B	Aristarchus Plateau 2	1.020	9.048	.734	.432	
5C	Aristarchus Plateau 3	1.019	8.802	.746	.458	

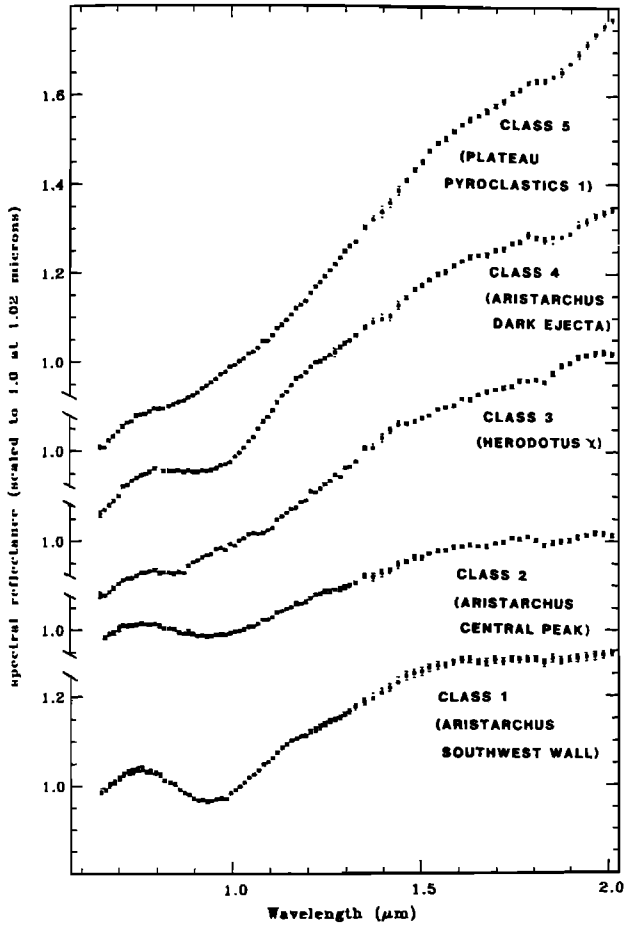

Fig. 5a

Fig. 5. (*a*) Representative spectra from each spectral class. The spectra are relative to the sun, normalized to 1.0 at 1.02 μm, and offset. (*b*) The same spectra relative to a straight line continuum as defined in the text.

to detect in assemblages with olivine. If possibility (4) is correct, the feldspar to mafic ratio could range from 3 to 0. The interpretation of Class 2 spectra, which best fits the spectral parameters, is an assemblage of clinopyroxene and olivine that has been brecciated, or contains feldspar at an abundance up to 70%, or both.

This class is not due to mixing of Class 1 material with either Class 3 or Class 5 because Class 2 has a shallower continuum slope than any of these. The maturing of Class 1 would also produce steeper continuum slopes than observed for Class 2.

Class 3

Interpretation: olivine and probable feldspar. The spectra of the south rim of Aristarchus and the mountain Herodotus X form this class (Figures 6*e,f*). They exhibit steeper continuum slopes than the Aristarchus interior spectra and very broad shallow bands centered beyond 1 μm. The two spectra differ somewhat in continuum slope and band depth perhaps because of minor compositional or maturity differences or contamination with surrounding terrain. The area for which the south rim spectrum was obtained includes the rim crest and deposits immediately interior and exterior to the crater. Herodotus X is an elongated (5 × 7 km) mountain in the northwestern portion of the plateau. This feature is surrounded by terrain blanketed with dark mantle material. Although the aperture was centered on the bright peak, very minor amounts of mantled terrain were included in the observation.

The mineral assemblage is spectrally dominated by olivine. The abundance of olivine relative to pyroxene could range from 80–100 wt %. The noise in the data prohibits eliminating pyroxene at less than about the 20 wt % level. Because the spectral signature of feldspar is very weak and occurs very near the broad olivine absorption, its abundance could be as high as 70% or as low as 0%. The high albedo of the olivine dominated units may require the presence of abundant feldspar [*Pieters and Wilhelms*, 1985].

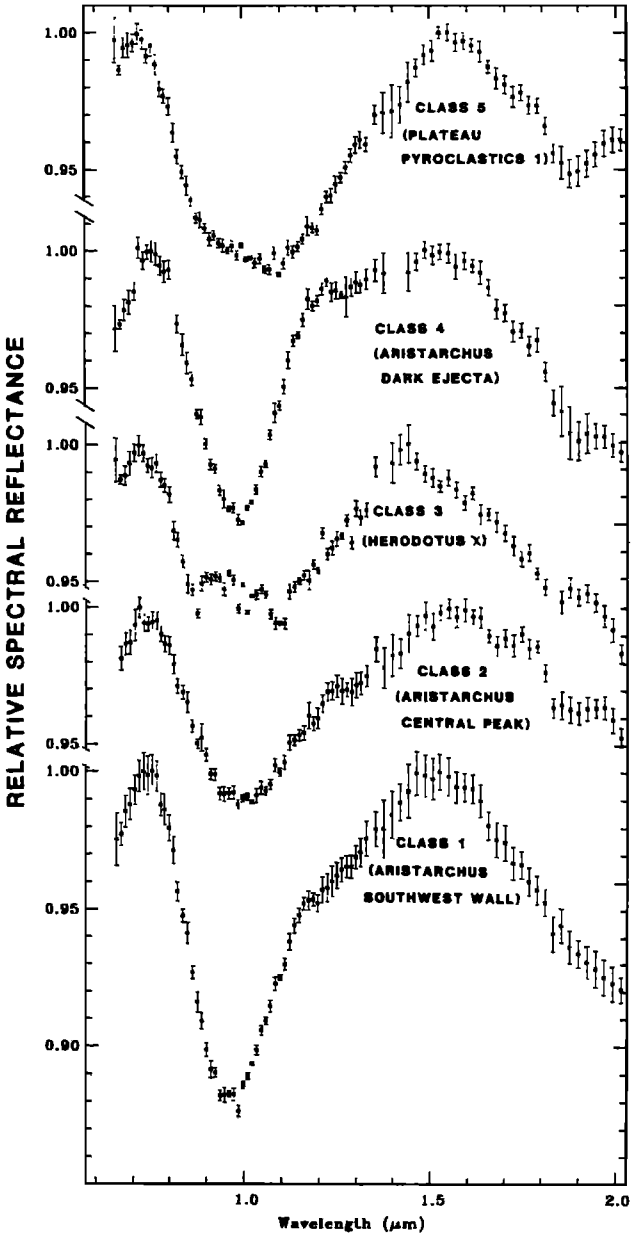

Fig. 5b

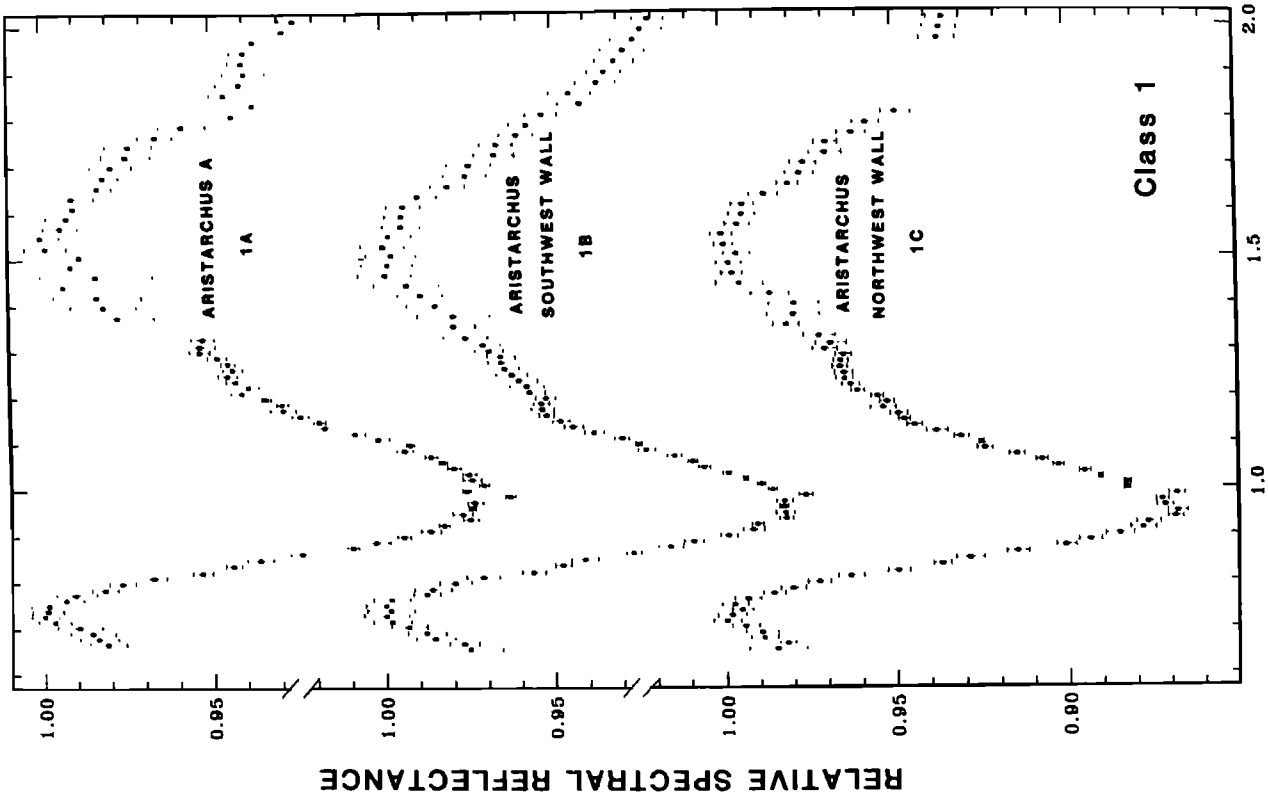

Fig. 6b

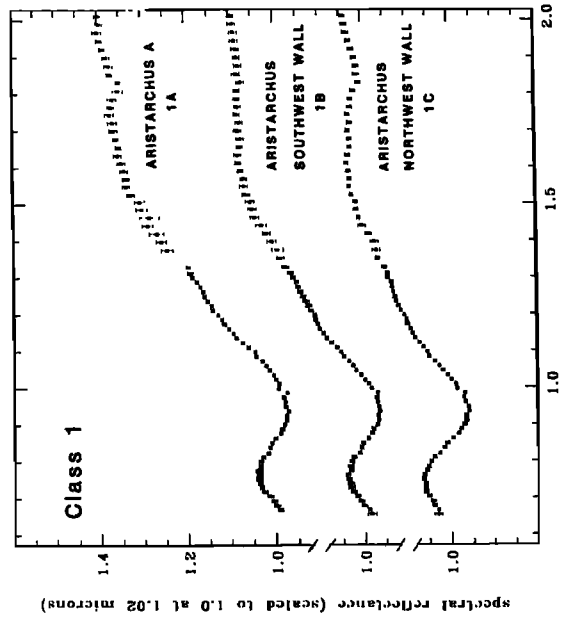

Fig. 6a

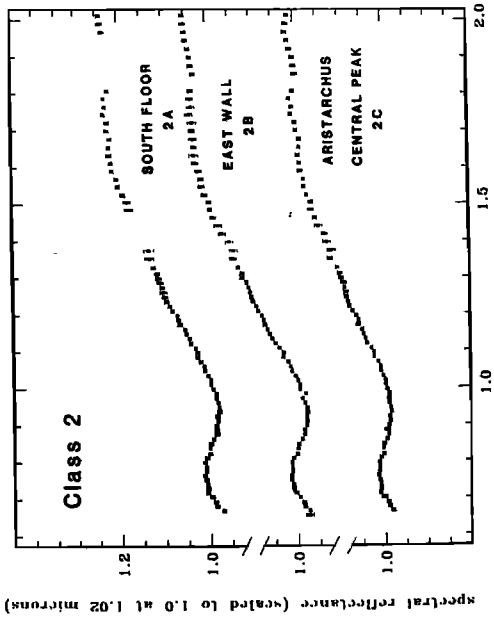

Fig. 6c

Fig. 6. (*a,c,e,g, and i*) The spectra of Classes 1 through 5 relative to the sun, normalized to 1.02 μm, and offset. The numbers and letters correspond to the class and member designations in Table 1 and Figure 3. (*b,d,f,h, and j*) The same spectra relative to a straight line continuum as defined in the text.

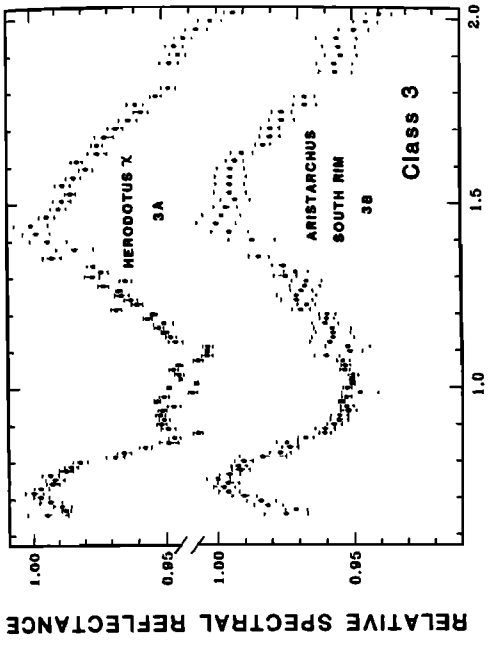

Fig. 6f

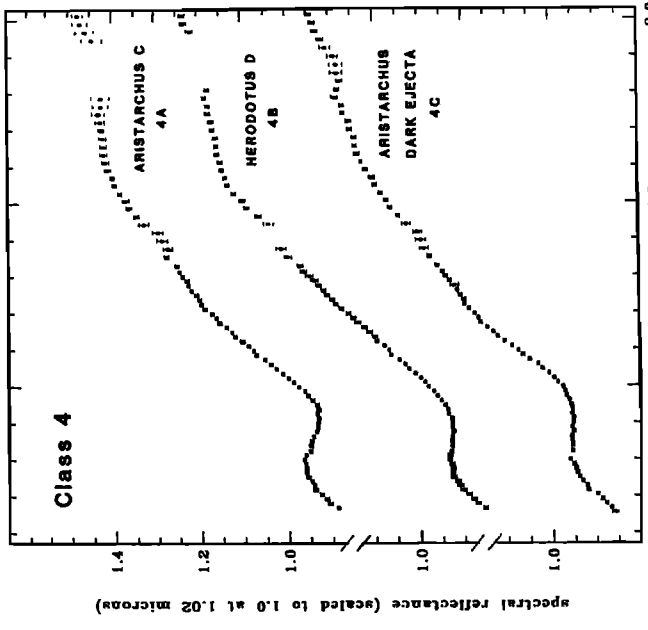

Fig. 6g

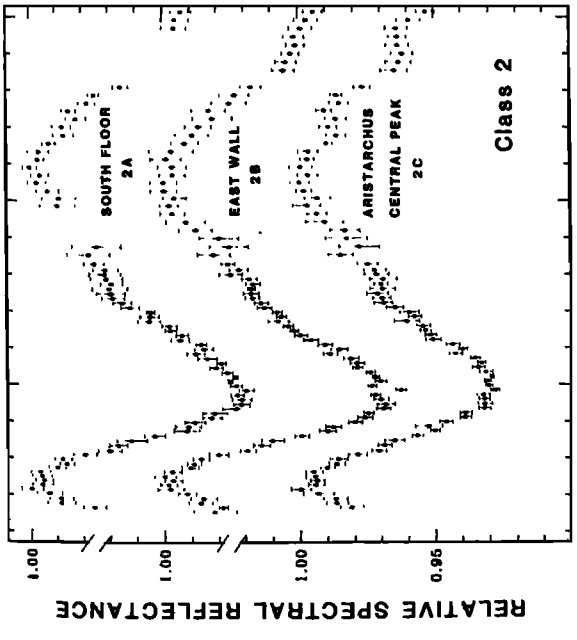

Fig. 6d

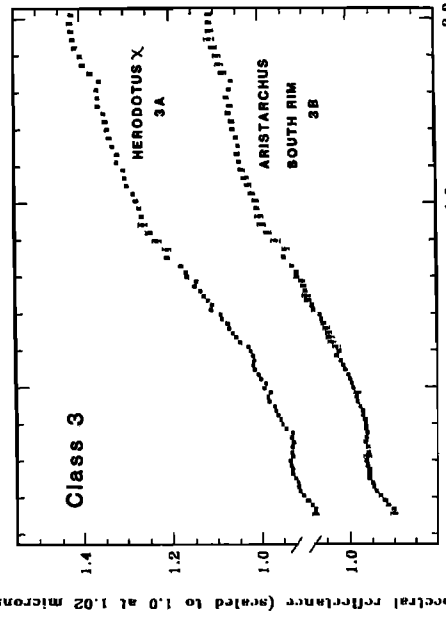

Fig. 6e

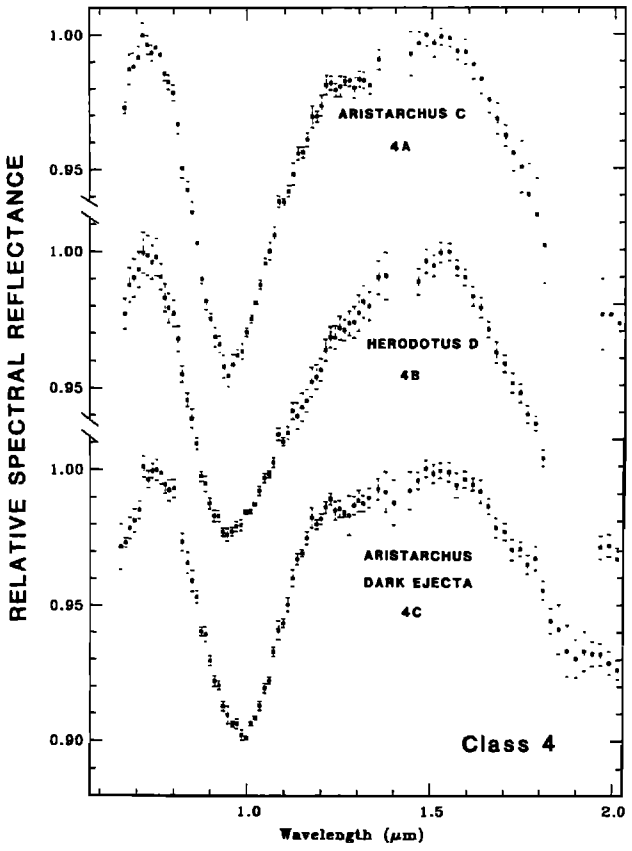

Fig. 6h

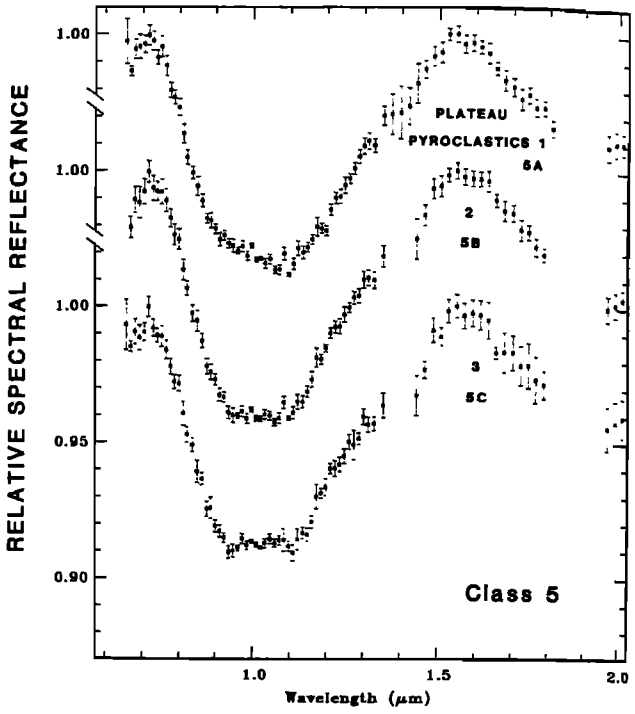

Fig. 6j

Class 4

Interpretation: materials with significant mare contamination. The spectra of the small craters Herodotus D and Aristarchus C and the dark ejecta deposit northeast of Aristarchus compose Class 4 and are shown in Figures 6*g,h*. With continua removed the band shapes of all these spectra are different and thus probably represent different compositions. Aristarchus C and Aristarchus dark ejecta share similar feldspar absorptions and band shapes but differ in band strength and wavelength of relative band minima. Aristarchus C and Herodotus D share similar relative absorption minima, yet the overall band shapes differ.

The geologic settings and detailed spectral characteristics, albedo, wavelength of relative band minima, and band shape suggest that no genetic relationship exists between the members of this class. However, the spectral characteristics of these locations are similar to those of mare areas [*Pieters et al.*, 1980], which suggests that each occurrence of this class has a significant, but difficult to quantify, component of mare material in the observed site.

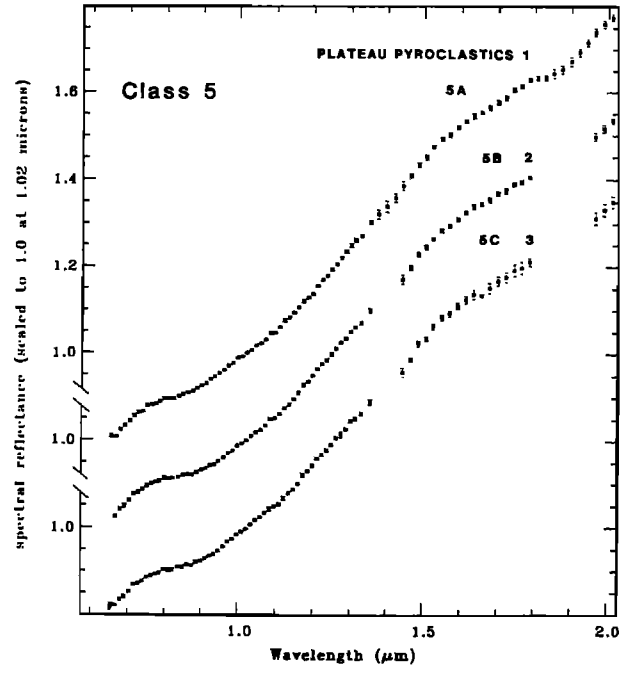

Fig. 6i

Class 5

Interpretation: pyroclastic glass. Spectra of the three dark mantle deposits observed share nearly identical characteristics, having steep infrared continua, low albedoes, and very broad absorptions centered longward of 1 μm (Figures 6*i,j*). These characteristics have been attributed to Fe^{2+}-bearing glass [*Hawke et al.*, 1983]. This material is essentially pure with other species present at less than 10 wt % and more probably 5 wt %. Because of the distinctly strong glass band these cannot be devitrified glasses such as Apollo 17 black spheres nor can they be similar to undevitrified glasses such as orange glass due to their very low albedo. The vitreous dark pyroclastic deposits occur both on the plateau and on portions of the surrounding mare deposits. The substrate has not affected the spectral characteristics of the dark mantle material.

IV. DISCUSSION

The near-IR reflectance data presented here address several scientific problems. The identification of three probable highlands assemblages, olivine or olivine-feldspar, augite-feldspar, and probably augite-olivine or augite-olivine-feldspar, at Aristarchus and on the plateau attests to the diversity of the highland crust beneath the mare basalts and the dark mantle. The extreme uniformity of widely separated pyroclastic deposits stands in marked contrast to the terra crustal heterogeneity. Lastly, the occurrence of mare-bearing material in the ejecta of Aristarchus but the lack of evidence mare basalt within the crater provides information on the stratigraphy of the target site.

Spectral classes 1, 2, and 3 appear to represent three crustal lithologies in the region. These compositions are consistent with the presence of an excavated plutonic complex. According to the nomenclature of *Stöffler et al.* [1980] and using the relative abundances of minerals derived from the reflectance spectra, Class 3 has a composition ranging from dunite to troctolite and would represent the material excavated from the deepest section of the pluton. The favored interpretation of Class 2 suggests a slightly shallower layer, this composition ranging from peridotite to, and traversing the entire field of, olivine gabbro. Class 1 would represent the shallowest material yet identified, having a rock type that ranges from gabbro through anorthositic gabbro to gabbroic anorthosite. The Th anomaly could be due to a property of one of these compositions, or to a thin incompatible zone that has not yet been spatially resolved.

A second possibility is deemed less likely but should be mentioned. The interpretation of the mineralogy of Class 2 can correspond to the rock type peridotite. If this is the case, the Aristarchus region may be a site where material from the lunar mantle is exposed at the surface.

In contrast to the highland compositions present in the region, the pyroclastics show marked uniformity despite the distances separating the locations. The spectra of pyroclastics in this region are distinct from those of other regions (with the possible exception of Mare Humorum pyroclastics) in the strength and symmetry of the 1-μm absorption [*Gaddis et al.*, 1985]. These absorption characteristics have been attributed to Fe^{2+}-bearing glass, which can have only minor amounts of other absorbing phases [*Hawke et al.*, 1983].

Previous mapping efforts [e.g., *Zisk et al.*, 1977] have indicated that Aristarchus crater straddled the mare-plateau boundary. The spectral data indicate that the Aristarchus cratering event penetrated the mare. No spectrum obtained within the crater can be interpreted as being mare-like. The spectral data presented here do not support earlier suggestions that the crater floor was covered with high-Ti basalt [*Zisk et al.*, 1977] or that the crater did not penetrate the mare [*Whitford-Stark and Head*, 1980]. The spectrum of the northern dark ejecta deposit provides positive evidence for the presence of mare in the target site. The spectrum of the dark ejecta deposit is like those of fresh mare craters [*Pieters et al.*, 1980]. This spectral mare affinity suggests that the dark deposit contains a large component of the mare basalt that existed in the upper portion of the southeastern half of the target site. The radial asymmetry of color units around Aristarchus has been noted [*Lucey et al.*, 1981]. The geologic units mapped by *Guest and Spudis* [1985] on the rim of Aristarchus also show radial asymmetry. The units' morphologic characteristics have been attributed to differences in the competence of the target materials between the mare to the east and the plateau to the west. These data suggest that mare basalt was ejected to the southeast of the mare/plateau contact.

V. CONCLUSION

The Aristarchus Plateau is extremely compositionally heterogeneous. Analysis of near-IR reflectance spectra has yielded three likely highland crustal compositions in the region: an olivine or olivine-feldspar assemblage, a clinopyroxene-feldspar mineral assemblage, and a probable clinopyroxene-olivine-feldspar assemblage. The thorium anomaly centered on Aristarchus crater may be correlated with one of the clinopyroxene-bearing mineralogies.

The pyroclastic deposits in the region show extreme homogeneity though their areal extent is of several tens of thousands of square kilometers [*Gaddis et al.*, 1985]. The spectra are indicative of uncrystallized Fe-Ti glass with an Fe^{2+} absorption.

The Aristarchus impact event fully penetrated the mare as shown by the lack of evidence of mare material inside the crater. However, mare material was present in the target site as shown by the mare affinities of the dark ejecta deposit north of the crater.

Acknowledgments. This work was carried out at the Hawaii Institute of Geophysics, University of Hawaii, under NASA grants NAGW 237, NSG 7312, and NSG 7323, which are gratefully acknowledged. Thanks are due to the scheduling committee of the University of Hawaii 2.2-m telescope for providing the observing time that allowed these spectral data to be obtained. P. Owensby provided valuable assistance in data collection and reduction. Very helpful reviews and comments were provided by P. Spudis, G. Ryder, and P. Warren. Images were provided by the Pacific Regional Planetary Data Center.

REFERENCES

Adams, J. B., Visible and near-infrared diffuse reflectance spectra of pyroxenes as applied to remote sensing of solid objects in the solar system, *J. Geophys. Res., 79*, 4829–4836, 1974.

Adams, J. B., and T. B. McCord, Electronic spectra of pyroxenes and interpretation of telescopic spectral reflectivity of the Moon, *Proc. Lunar Sci. Conf. 3rd*, 3021–3034, 1972.

Cameron, W. S., Comparative analyses of observations of lunar transient phenomena, *NASA TM-X-65528*, 85 pp., 1971.

Charette, M. P., T. B. McCord, C. M. Pieters, and J. B. Adams, Applications of remote spectral reflectance measurements to lunar geology, classification, and determination of titanium content of lunar soils, *J. Geophys. Res., 79*, 1605–1613, 1974.

Clark, R. N., A large scale interactive one-dimensional array processing system, *Pub. A.S.P., 92*, 221–224, 1979.

Crown, D. A., and C. M. Pieters, Spectral properties of plagioclase and pyroxene mixtures (abstract), in *Lunar and Planetary Science XVI*, pp. 158–159, Lunar and Planetary Institute, Houston, 1985.

Davies, D. W., T. V. Johnson, and D. L. Matson, Lunar multispectral imaging at 2.26 μm: First results, *Proc. Lunar Sci. Conf. 10th*, 1819–1827, 1979.

Etchegaray-Ramirez, M. I., A. E. Metzger, E. L. Haines, and B. R. Hawke, Thorium concentrations in the lunar surface: I.V. Deconvolution of the Mare Imbrium, Aristarchus, and adjacent regions, *Proc. Lunar Planet. Sci. Conf. 13th*, in *J. Geophys. Res., 87*, A529–A543, 1982.

Gaddis, L. R., C. M. Pieters, and B. R. Hawke, Remote sensing of lunar pyroclastic mantling deposits, *Icarus, 61*, 461–489, 1985.

Gaffey, M. J., Spectral reflectance characteristics of the meteorite classes, *J. Geophys. Res., 81*, 905–920, 1976.

Gorenstein, P., and P. Bjorkholm, Detection of radon emanation from the crater Aristarchus by the Apollo 15 alpha particle spectrometer, *Science, 179*, 792–794, 1973.

Guest, J. E., Stratigraphy of ejecta from the lunar crater Aristarchus, *Geol. Soc. Am. Bull., 84*, 2873–2894, 1973.

Guest, J. E., and P. D. Spudis, The Aristarchus impact event and the effects of target material, *Geol. Mag.*, in press, 1985.

Haines, E. L., M. I. Etchegaray-Ramirez, and A. E. Metzger, Thorium concentrations in the lunar surface: III. Deconvulation of the Apennines region, *Proc. Lunar Planet. Sci. Conf. 10th*, 1701–1718, 1979.

Hawke, B. R., P. G. Lucey, T. B. McCord, C. M. Pieters, and J W. Head, Spectral studies of the Aristarchus Region: Implications for the composition of the lunar crust (abstract), in *Lunar and Planetary Science XIV*, pp. 289–290, Lunar and Planetary Institute, Houston, 1983.

Lucey, P. G., B. R. Hawke, C. M. Pieters, and T. B. McCord, Multispectral unit mapping of the Aristarchus region of the Moon, *Bull. Am. Astron. Soc., 13*, 711, 1981.

McCord, T. B., R. N. Clark, B. R. Hawke, L. A. McFadden, P. D. Owensby, C. M. Pieters, and J. B. Adams, Remote detection of olivine, pyroxene, and plagioclase: Analysis of three lunar site (abstract), in *Lunar and Planetary Science XII*, pp. 679–681, Lunar and Planetary Institute, Houston, 1981.

Moore, H. J., Geologic map of the Aristarchus region of the Moon, *U.S. Geol. Surv., Geol. Invest. Map I-465*, 1965.

Moore, H. J., Geological map of the Seleucus Quadrangel of the Moon, *U.S. Geol. Surv., Geol. Invest. Map*, I-527, 1967.

Nash, D. B., and J. E. Conel, Spectral reflectance systematics for mixtures of powdered hypersthene, labradorite, and ilmenite, *J. Geophys. Res., 79*, 1615–1621, 1974.

Pieters, C. M., S. Flam, and T. B. McCord, Near infrared lunar spectra: Patterns in the increasing data set (abstract) in *Lunar and Planetary Science XI*, pp. 879–881, Lunar and Planetary Institute, Houston, 1980.

Pieters, C. M., and D. E. Wilhelms, Origin of olivine at Copernicus, *Proc. Lunar Planet. Sci. Conf. 15th*, in *J. Geophys. Res., 90*, C415–C420, 1985.

Shorthill, R. W., and J. W. Saari, Non-uniform cooling of the eclipsed Moon: A list of thirty prominent anomalies, *Science, 50*, 210–212, 1965.

Stöffler, D., U. B. Marvin, C. H. Simonds, and P. H. Warren, Recommended classifcation and nomenclature of lunar highland rocks—a committee report, in *Proceedings of the Conference on the Lunar Highlands Crust*, pp. 51–70, edited by J. J. Papike and R. B. Merrill, Pergamon, New York, 1980.

Thompson, T. W., A review of earth-based radar mapping of the Moon, *Moon and Planets, 20*, 179-198, 1979.

Whitaker, E. A., G. P. Kuiper, W. K. Hartmann, and L. H. Spradley, *Rectified Lunar Atlas: Supplement B to the Photographic Lunar Atlas*, xx pp. University of Arizona Press, Tucson, 1963.

Whitford-Stark, J. L., and J. W. Head, Stratigraphy of Oceanus Procellarum basalts: Sources and styles of emplacement, *J. Geophys. Res., 85*, 6579–6609, 1980.

Wood, R. W., Selective absorption of light on the Moon's surface and lunar petrography, *Astrophys. J., 36*, 75, 1912.

Zisk, S. H., C. A. Hodges, H. J. Moore, R. W. Shorthill, T. W. Thompson, E. A. Whitaker, and D. E. Wilhelms, The Aristarchus-Harbinger region of the Moon: Surface geology and history from recent remote sensing observations, *Moon, 17*, 59–99, 1977.

P. G. Lucey, B. R. Hawke, and T. B. McCord, Planetary Geosciences Division, Hawaii Institute of Geophysics, 2525 Correa Road, Honolulu, HI 96822.

C. M. Pieters and J. W. Head, Department of Geological Sciences, Brown University, Providence, RI 02912.

(Received May 17, 1985;
revised September 25, 1985;
accepted October 29, 1985.)